Research Article

Effects of Parameters on Heat Transfer Characteristics of a Rectangular Cross-Section Heat Pipe with Mesh Wick

Surachet Sichamnan
The Thermal System Research Unit (TSR), Department of Mechanical Engineering, Faculty of Industry and Technology, Rajamangala University of Technology Isan, Sakon Nakhon Campus, Sakon Nakhon, Thailand

Anurak Rodbumrung*
Faculty of Industrial Technology, Rambhai Barni Rajabhat University, Chanthaburi, Thailand

* Corresponding author. E-mail: anurak.ro@rbru.ac.th DOI: 10.14416/j.asep.2021.11.010
Received: 12 May 2021; Revised: 22 June 2021; Accepted: 10 August 2021; Published online: 24 November 2021

Abstract
This research investigated the effects of parameters on heat transfer characteristics of a rectangular cross-section heat pipe with mesh wick (RHP/MW). The working substance used Distilled Water and Refrigerant R-11. Heat loads at the evaporator were set at 20, 40, 60, and 80 W. Results revealed that, throughout the test, RHP/MW/R11 gave the highest heat transfer rate and average heat flux of 26.91 W and 2054.57 kW/m^2, respectively. Heat Load of 80 W produced the lowest total thermal resistance of 0.4388 °C/W with the highest average thermal efficiency of 52.91%, the highest efficiency among the test cases. This is due to an increase of heat receiving areas of RHP/MW. More heat is transferred through the pipe wall to the wet perimeter of the working substance which caused the working substances in the evaporator to boil faster. The mesh wick also helped the condensed working substance to disperse around the inner tube wall and resulted in a thin film of the condensate liquid. This resulted in a higher heat transfer rate and heat flux for the RHP/MW. Mesh wick also generated capillary pressure that drew the condensed liquid back to the evaporator. The maximum capillary pressure obtained from the test was 93.29 N/m^2 when the heat load of 80 W was applied to the RHP/MW/R11. RHP/MW/R11 greatly enhances the heat transfer characteristics. Thus, it is suitable for application as an alternative to specific work sites that require smooth contact with heat receiving areas.

Keywords: Rectangular heat pipe, Mesh wick, Heat transfer, Capillary pressure

1 Introduction

Industrial and technological growth are important factors in the economic development in the modern world. The utilization of natural resources in many industrial systems has resulted in adverse effects on the environment. Therefore, each step of the industrial process should be carefully considered. Most industrial processes produce residual energy, such as hot air, hot water, hot steam, cold air, cold water, and cold steam. Having a device that can renew these energies will maximize the industry process and its efficiency as well as reduce the costs by using natural resources as starting agents. A heat pipe is a type of heat exchanger that can transfer heat from a heat source to a heat sink without relying on external energy to operate.

The heat pipe with a mesh wick as shown in Figure 1(a) is divided into three sections: evaporator section, adiabatic section, and condenser section. The internal wall of the pipe is covered by mesh wick. To operate, the heat pipe relies on the latent heat of the working substance contained within the evaporator, which receives heat from a heat source until the saturated liquid evaporates. Then, the latent heat-vaporized working substance travels to the condenser where heat transfer occurs as a result of condensation. This

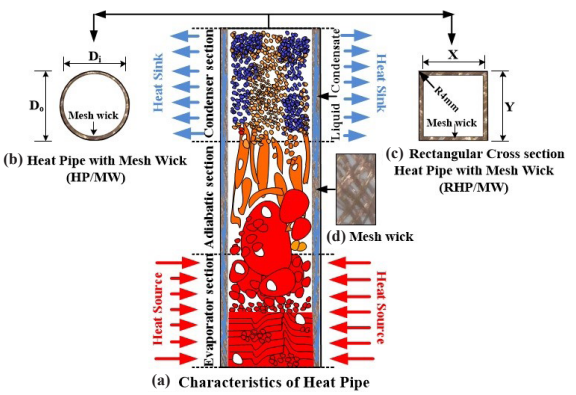

Figure 1: (a) Characteristics of a heat pipe with mesh wick, (b) mesh-wicked heat pipe, (c) RHP-MW, and (d) mesh wick.

allows large amounts of heat to be transferred from the evaporator to the condenser end, even with a slight temperature difference [1]. The mesh wick mounted on the inner wall of the heat pipe contains a gap in the middle as shown in Figure 1(a). This allows the vapors from the evaporator to move towards the condenser. Mesh wick's porosity also creates a capillary force that has a high permeability. Therefore, the heat pipes can transfer heat horizontally while pulling the condensed working substance back to the evaporator. This type of heat exchanger possesses a high heat transfer rate [2], [3]. On the other hand, a thermosyphon (TPCT) that does not have a mesh wick relies on Earth's gravity to draw the condensed working substance in the liquid state back to the evaporator. Furthermore, counterflow, the collision between the working substance in liquid and vapor states within the evaporator, and the inability to operate in a horizontal position limit the usage of TPCT. The applications and efficiency of heat transfer by heat pipes have been continuously improved. These developments include: the optimization of solar panels using heat pipes fitted with a copper mesh wick [1], reducing the temperature of the incoming air before reaching an air conditioner's condenser [4], as well as cooling electronic equipment [5]. Moreover, the applications have also been used in factory and industrial heat exchangers [6] along with determining the effectiveness of Close End Flat Heat Pipe Heat Exchangers (CEFHPHE) [7]. Further studies also include the use of silver nanoparticles as a working substance to improve the heat transfer efficiency of a heat pipe equipped with a mesh wick [8]. Using Titanium nanoparticles as a working substance to determine the thermal efficiency of the pipe [9], enhancing the thermal performance of a flat micro heat pipe with a rectangular grooved wick using nanoparticle fluid as a working substance [10].

Considering the research data and the nature of the past applications, heat pipes are mostly circular or flat cross-sectional types. Research on the modification of the physical structure of heat pipes is limited. Therefore, further development and application of mesh wick in heat pipe offer future research opportunities. In this research, the mesh wick was installed on a rectangular tube to create a rectangular heat pipe with a mesh wick (RHP/MW) as shown in Figure 1(c). Due to the properties of the mesh wick which contributes to the division and reduction of collisions between the active substance in the vapor and the liquid state, when the liquid flows through the mesh wick part of the heat pipe which causes low flow velocity and high viscosity. This results in low shear stress and shear rate, which is the flow behavior of the working substance in the smaller pipes. This is considered a normal flow pattern for the case of fluid flowing through the mesh wick of the heat pipe [2].

The research focused on the effect of heat load and working substance on heat transfer rate, heat flux, the difference of water outlet and inlet temperatures at the condenser, the wall temperature distributions, total thermal resistance, and RHP/MW's thermal efficiency. Expected results were the effects of heat load and working substance on heat transfer rate, heat flux, the difference of water outlet and inlet temperatures at the condenser, the wall temperature distributions, total thermal resistance, and RHP/MW's thermal efficiency. The obtained results will serve as a basis for future development and applications of RHP/MW in the future.

2 Materials and Methods

2.1 *Characteristics of cross-section modification and installation of mesh wicks*

The cross-section modification as shown in Figure 2 exhibits the fundamental relationship, such as the cross-sectional area, wet contact perimeter, and hydraulic radius [11]–[13].

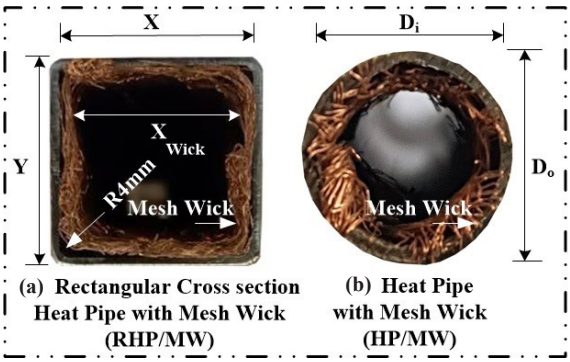

Figure 2: Characteristics of the cross-sectional geometry, installation of mesh wick, and heat receiver surface areas in RHP/MW and HP/MW.

Cross-sectional area A_c can be calculated from Equation (1)

$$A_c = \frac{\pi Y^2}{4} + (XY) \tag{1}$$

Wet perimeter ($W_{primeter}$), Hydraulic radius (R_h) can be calculated from Equations (2) and (3)

$$W_{primeter} = \pi Y + 2X \tag{2}$$

$$R_h = \frac{(\pi/4)Y^2 + (XY)}{\pi Y + 2X} = \frac{A_c}{W_{perimeter}} \tag{3}$$

Where Y and X are the outer and inner distances of the rectangular pipe (m), respectively, D_o and D_i are the outer and inner diameter of the round pipe (m), as shown in Figure 2. When compare between RHP/MW and HP/MW, Hydraulic radius (R_h) is determined with the same value of 0.0068 (m) as per Equation (3).

Mesh wicks also helped to disperse the condensed liquid and spread it across the condenser surface, and reduce the thickness of the liquid film created by the condensation. This resulted in a better transfer of heat to the heat receiver. Mesh wicks can spread liquids around the evaporator surface where heat is passed through the heat pipe by conduction of heat from the heat source. The heat must flow through the mesh wick into the working substance radially. The mesh-type mesh wick used in this test was made of copper wire which has good thermal conductivity. When the radial temperature was slightly reduced, the working substance boiled rapidly. Thermal conductivity and the effectiveness of the mesh wick are calculated from Equation (4) [2], [3].

$$k_{wick} = \left(\frac{\beta - \varepsilon}{\beta + \varepsilon}\right) k_1 \tag{4}$$

Where, $\beta = \left(1 + \frac{k_s}{k_l}\right) / \left(1 - \frac{k_s}{k_l}\right)$, k_s is the thermal conductivity of the mesh wick, ($W/m \cdot °C$), k_1 is the thermal conductivity of the working substance, ($W/m \cdot °C$) and ε is the gap by volume of the mesh wick.

The mesh wick inside the heating pipe also creates capillary pressure that draws the condensed liquid back into the evaporator. Hence, the liquid could absorb more heat from the heating source again. The capillary pressure of the mesh wicks (P_c) is calculated from Equation (5).

$$P_c = \frac{2\sigma_l}{r_e} \tag{5}$$

Where σ_l is the surface tension of the working substance (N/m), r_e is the pore radius of the mesh wick (m).

2.2 *Heat transfer rate and heat flux*

The heat transfer in the (RHP/MW) begins when the working substance, a saturated liquid state contained in the evaporator, is heated, boiled, and vaporized. Then, the vapor floats through the heat shield to release the heat at the condenser and change from vapor to liquid. The mesh wick mounted on the inside of the pipe wall created capillary pressure to draw condensed liquid back into the evaporator. This mechanism and the Earth's gravity help the fluid return to the evaporator chamber. The heat transfer rate and heat flux can be calculated from Equations (6) and (7), respectively [14], [15].

The heat transfer rate and heat flux are calculated from Equations (6) and (7) as,

$$Q = \dot{m} C_p \left(T_{co} - T_{ci}\right) \tag{6}$$

$$q = \frac{Q}{A_{cond}} \tag{7}$$

Which Q is the heat transfer rate, (W), $\dot{m}$ is the water flow rate at the condensation, kg/s, C_p is the specific heat capacity of the water at the condensation,

($J/kg \cdot °C$), T_{co} is the temperature of the outlet water at the condensation, ($°C$), T_{ci} is the temperature of the water inlet at the condenser ($°C$), q is the heat transfer rate, (Wm^2), A_{cond} is the pipe surface area in the condenser (m^2) .

2.3 *Surface temperature of the tube's inner wall at the evaporator and condenser*

These temperatures are calculated from Equations (8) and (9) [11]–[13], [15].

$$T_{ei} = T_{eo} - \frac{Q \ln(Y/X)}{2\pi k_{wall} L_e} \tag{8}$$

$$T_{ci} = T_{co} - \frac{Q \ln(Y/X)}{2\pi k_{wall} L_c} \tag{9}$$

Where K_{wall} is the thermal conductivity of the pipe wall, ($W/m \cdot °C$), L_e is the length of the pipe at the evaporator, (m), L_c is the length of the pipe at the condenser, (m), D_o and D_i are the outer and inner diameter of the round pipe (m) respectively, Y and X are the outer and inner length of the rectangular pipe (m), meaning $Y = D_o$, $X = D_i$ respectively, see Figure 2.

2.4 *The total thermal resistance*

The combined heat resistance between the evaporator and the condenser can be calculated from Equation (10) [16]

$$Z = \frac{T_{ei} - T_{ci}}{Q_{in}} \tag{10}$$

Where Z is the total thermal resistance, ($W/°C$) means $Z = Z_2 + Z_3 + Z_7 + Z_8$ [17] and Q_{in} is the Heat Load to the evaporator section (W) for which Q_{in} is calculated from Equation (11) [8], [18]

$$Q_{in} = VI \tag{11}$$

Where V is the Voltage of the heater, (V) and I is the current that was passed to the heater (A). The thermal resistances that occurred on the pipe wall at the evaporator (Z_2) and condenser (Z_8) are as shown in Figure 3, together with Equations (12) and (13) [2], [3], [17].

$$Z_2 = \frac{\ln(Y/X)}{2\pi k_{wall} L_e} \tag{12}$$

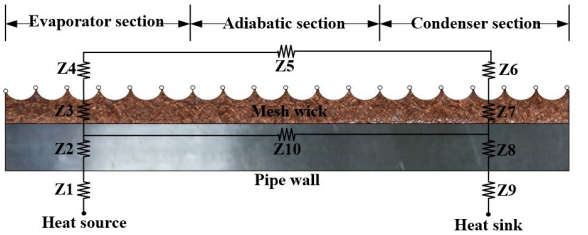

Figure 3: Thermal resistance circuit with mesh wicks.

$$T_{ci} = T_{co} - \frac{Q \ln(Y/X)}{2\pi k_{wall} L_c} \tag{13}$$

Heat resistance of the mesh wick at the evaporator and condensers can be determined from Equations (14) and (15) [2], [3], [17].

$$Z_3 = \frac{\ln(X/X_{wick})}{2\pi k_{wick} L_e} \tag{14}$$

$$Z_7 = \frac{\ln(X/X_{wick})}{2\pi k_{wick} L_c} \tag{15}$$

Where X and Y are the inner and outer length of the rectangular pipe (m), K_{wall} is the thermal conductivity of the pipe wall, ($W/m \cdot °C$), L_e is the length of the pipe at the evaporator, (m), L_c is the length of the pipe at the condenser, (m), X_{wick} is the inner length of the mesh wick (m), X_{wick} is the thermal conductivity of the mesh wick ($W/m \cdot °C$), meaning $Y = D_o$, $X = D_i$ respectively, see Figure 2.

2.5 *Thermal performance*

Thermal efficiency can be calculated from Equation (16) [19].

$$\eta = \frac{Q_c}{Q_e} = \frac{Q}{Q_{in}} \tag{16}$$

Where η refers to thermal efficiency, Q is heat transfer rate (W), and Q_{in} is Heat Load to the evaporator section.

Furthermore, Thermal efficiency can be expressed as per Equation (16) and Heat transfer rate as per Equation (1). The energy balance equation at the evaporator Q'_{evap} [20] was designed to have no heat loss at the insulation as per Equation (17).

$$Q'_{evap} = Q_{evap} - Q_{insul} - Q_{wall} \tag{17}$$

When $Q_{evap} = Q_{in} = VI$ is shown in Equation (11) and Q_{insul} is the heat loss through the insulation, (W) as calculated from Equation (18).

$$Q_{insul} = A_{insul} h_{insul,o} (T_{insul,o} - T_{envi}) \quad (18)$$

When A_{insul} is the area of insulation, (m^2). $h_{insul,o}$ is the outer insulation average heat transfer coefficient, ($W/m \cdot °C$) and $T_{insul,o}$ are T_{envi} the average temperature of the outer surface of the insulation and the environment ($°C$), respectively.

For Q_{wall} this is determined by the heat loss due to the heat transfer through the tube's surface as per Equation (19)

$$Q_{wall} = Q_{conduction} = K_{wall} A_{evap} \Delta T_{evap} \quad (19)$$

When K_{wall} is the thermal conductivity of the pipe wall, ($W/m \cdot °C$). A_{evap} is the area of the heat pipe at the evaporator, (m^2). ΔT_{evap} is the average temperature difference between the outer and inner surface of the heat pipe at the condenser ($°C$).

2.6 *Uncertainty analysis of measured parameters*

The uncertainty of the heat transfer rate is calculated using Equation (20) [8].

$$\frac{\Delta Q}{Q} = \left[\left(\frac{\Delta V}{V}\right)^2 + \left(\frac{\Delta I}{I}\right)^2 + \left(\frac{\Delta L_e}{L_e}\right)^2 + \left(\frac{\Delta d_e}{d_e}\right)^2 \right]^{1/2} \quad (20)$$

This is calculated from the uncertainties of the Voltage of the heater (ΔV) and the Current (ΔI) passing through the heater. It also includes the uncertainties due to the length (ΔL_e) and diameter (Δd_e) of the evaporator. The maximum uncertainty of the heat transfer rate was 4.32%. The uncertainty of the thermal resistance can be calculated from Equation (21) [8].

$$\frac{\Delta Z}{Z} = \left[\left(\frac{\Delta Q}{Q}\right)^2 + \left(\frac{\Delta(\Delta T)}{\Delta T_{EC}}\right)^2 \right]^{1/2} \quad (21)$$

Where ΔQ will depend on the uncertainty of the applied heat and the difference between the evaporator and the condenser $\Delta(\Delta T)$, and the actual measured temperature ΔT_{EC}. The maximum uncertainty obtained from the study was 5.33%

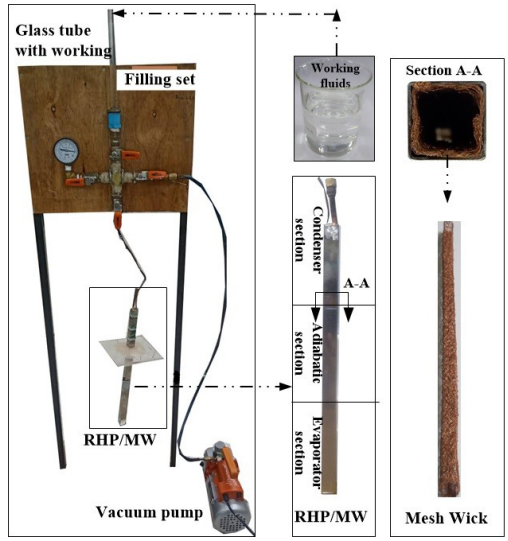

Figure 4: The process of constructing an RHP/MW.

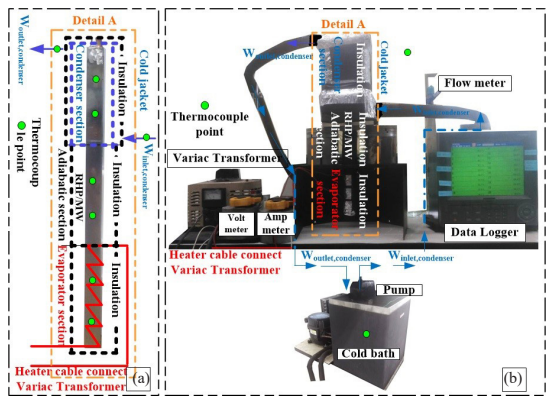

Figure 5: Installation of test equipment and test procedures.

2.7 *Equipment installation and testing*

The process of constructing an RHP/MW where the mesh wick was installed on the inner surface of the pipe, welding both ends of the pipe, and connecting the outlets to the vacuum and working substance feeding system through small pipes. RHP/MW was vacuumed by using the vacuum pump to extract all the air from inside the pipe. Then, the working substance was subsequently added to the RHP/MW using a filling vial as shown in Figure 4.

The installation of the test equipment and the test procedure is shown in Figures 5(a) and (b). At the RHP/MW's evaporator, a cable heater was wrapped around

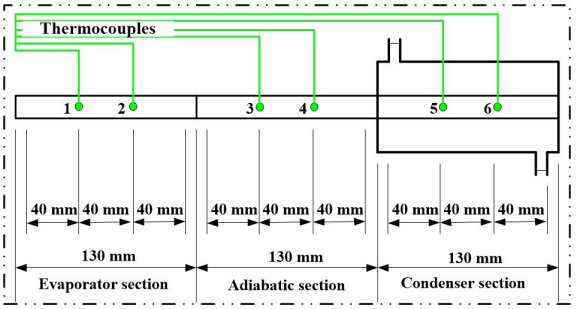

Figure 6: Positions of temperature measuring points.

the evaporator to provide heat and connected to the Variac Transformer to adjust the voltage according to the specified parameters. Variac Transformer was measured for its voltage and amps by another multimeter. Water was pumped from the chilled water bath through a flow meter to the condenser of the RHP/MW, which was covered by the cold jacket. Water from the condenser flowed to the chilled water bath again. There are 10 temperature measurement points, measured with a K-type thermocouple with an accuracy of ± 1.5 °C connected to a data logger (Yokogawa DX200) with an accuracy of ± 1 °C. These 10 measuring points consisted of: 2 on the pipe surface at the evaporator section, 2 on the surface of the adiabatic section, 2 on the pipe surface at the condenser section, 2 on the inlet and outlet water at the condenser section, 1 on the chilled water bath, and 1 on the external environment. The test parameters in this study are shown in Table 1 and the surface temperature measurement site on the heat pipe is shown in Figure 6. There are two measuring points at the evaporator at positions 1 and 2, two measuring points on the heat shield at positions 3 and 4, and two measuring points at the condenser at positions 5 and 6.

In terms of equipment installation and testing procedures, the heat transfer rate of the system can be calculated from Equation (22) [21]

$$Q_{system} = Q_{convection} + Q_{conduction} \quad (22)$$

Equation (23) is used to calculate the rate of heat conduction of the system.

$$Q = Q_{convection} = \dot{m} C_p (T_{co} - T_{ci}) \quad (23)$$

Now it becomes:

Table 1: Controlled and variable parameters

Conditions	
1. Independent Variable	1.1 Heat pipes, rectangular and round cross-sectional pipes with mesh wick (RHP/MW, HP/MW).
	1.2 Thermosyphon, rectangular, and round cross-sectional thermosyphons (RTPCT, TPCT) are used for comparison.
	1.3 The working substances used, water and R-11.
	1.4 Heat load at evaporator of 20, 40, 60, and 80 W.
2. Dependent Variables	2.1 The heat transfer rate and heat flux
	2.2 Temperature differences between the outlet water and inlet water at the condensation
	2.3 The wall temperature distributions
	2.4 Total thermal resistance and Thermal Performance
3. Control Variables	3.1 The heat pipe is made of stainless steel grade 304 (AISI 304).
	3.2 Mesh wick made of copper wire, wire diameter 0.1 mm, mesh frequency of 100 mesh and a void fraction (ε) is 0.948
	3.3 RHP/MW, RTPCT with the outer length of 20 mm on each side (Y), and 0.5 mm thickness.
	3.4 HP/MW, TPCT with an outer diameter of 20 mm (Do), and 0.5 mm thickness.
	3.5 Cross-sectional area after modification (Ac) is 0.00069 m^2.
	3.6 The wet parameter (Wprimete) is 0.10 m.
	3.7 Test angle of 90°
	3.8 Inlet water flow rate at condensate of 0.25 l / min.
	3.9 Inlet water temperature at the condensation of 25 °C
	3.10 Evaporator, heat shield, and condenser have the same length of 130 mm.
	3.11 The working substance filling rate is 50% of the volume of the evaporator.

$$Q = f(\dot{m}, T_{co}, T_{ci})$$

Heat loss is determined by the heat conduction through the pipe wall, which is analyzed by Engineering Sciences Data Unit Data Item No. 80013 (ESDU81038) [22]. The wall heat transfer rate loss was calculated using Fourier's law [23] as shown in Equation (24).

$$Q_{conduction} = K_{wall} A \Delta T \quad (24)$$

Thus,

$$Q = f(K_{wall}, A, \Delta T)$$

Where K_{wall} is the thermal conductivity of the pipe wall, ($W/m \cdot °C$). A is the area of the heat pipe, (m^2). ΔT is the difference between the average temperature of the pipe's surface temperatures at the evaporator and condenser (°C) respectively.

3 Results and Discussion

This research investigated the parameters affecting the heat transfer characteristics of (RHP/MW). The results are presented as follows

- Heat transfer rate and heat flux
- Temperature differences between the outlet water and inlet water at the condensation
- The wall temperature distributions
- Total thermal resistance and Thermal Performance

Abbreviations symbols

- Rectangular cross-section Heat Pipe with Mesh Wick, (RHP/MW)
- Heat Pipe with Mesh Wick, (HP/MW)
- Rectangular cross-section Two-Phase Closed Thermosyphon, (RTPCT)
- Two-Phase Closed Thermosyphon, (TPCT)
- Refrigerants-11, (R11)
- Distilled Water, (DW)

3.1 *Heat transfer rate and heat flux*

The relationship between the heat load at the evaporator and the heat transfer rate. An increase in heat load resulted in a higher heat transfer rate. At 80 W of heat load, the highest heat transfer rate was achieved in all test cases. RHP/MW/R11 shows a maximum heat transfer rate of 41.98 W. The structural characteristics of RHP/MW provide a greater contact area to receive the heat when compared to HP/MW as shown in Figure 7.

Therefore, from this study, the pipe surface temperature at the evaporator of the heat pipe, the cold water temperature of the inlet and outlet at the condensing of the heat pipe including tube surface temperature distribution in each heat pipe section is considered by referring to the heat load at evaporator of 20, 40, 60, and 80 W. Therefore, the steady-state system is ready to be examined and have the data in

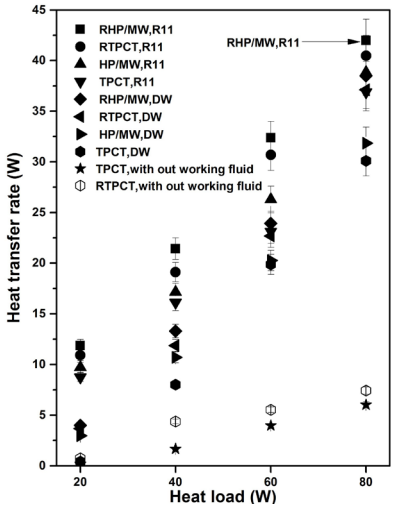

Figure 7: The relationship of heat load with heat transfer rate.

various parts recorded to determine the heat transfer rate and heat flux. The liquid working substance in the liquid state boils and vaporizes. When receiving enough heat from the heat source. Then, the vapor will flow through the heat shield to cool down at the condenser. The condensed liquid flows back to the evaporator, which forms a continuous cycle of operation as long as the evaporator is heated throughout the test.

As a result, the heat receiving area in the evaporator and the cooling at the condenser became greater as well. As the mesh wick in the evaporator allowed more heat from the heating source to be absorbed, the working substance within the RHP/MW's evaporator could easily boil and vaporize. When the heat from the heating source passed through the heat pipe wall, the heat flow through the mesh wick into the working substance radially. This resulted in a slight decrease in the radial temperature, allowing the working substance to boil rapidly. Furthermore, mesh wick also increased the contact area at the solid-liquid interface [19], which led to the initial nucleate boiling as well. In addition, the condensed vapor releases heat to the heat sink creates capillary pressure at the contact between the liquid and the vapor. This is due to the surface tension of the working substance and the menisci of the increased heat-emitting areas. Therefore, the condensed liquid was drawn through the pores of the mesh wick back to the evaporator [24]. This allowed the condensed liquid to spread around the inner wall

of the heat pipe, which reduced the counter-flow problem between the working substance in the vapor state from the evaporator and the working substance flowing back from the condenser [8], [16], [17] This phenomenon brings a large enough volume of the returning condensed liquid that can prevent the formation of hot spots. The mesh wick installed inside the heat pipe generates capillary pressure that drew the condensed liquid back to the evaporator. The maximum capillary pressure obtained from the test was 93.29 N/m^2, found in the RHP/MW/R11 at 80 W of heat load. When using working substances with high latent heat and low boiling points such as R11, RHP/MW's, the evaporator also creates vapor by heat transfer surface. This occurrence might be attributed to the temperature which increases with the heat load. Thus, this condition allows the heat transfer from the pipe wall to the working substance to increase as well. The active substance, which has a higher latent heat of vaporization and lower surface tension between the liquid-gas interface, along with a higher heat transfer coefficient, helps the vapor to move up for cooling at the condenser. This is consistent with every test result as shown in Figure 7. Upon comparing the heat transfer rate between RHP/MW/R11 and HP/MW/R11, or the comparison between RHP/MW/DW and HP/MW/DW, results showed that the rate of average heat transfer from RHP/MW was higher than the one from HP/MW. This is consistent with the physical structure characteristics of RHP/MW as previously described.

When considering the relationship of heat load and heat flux as shown in Figure 8, an increase in the heat load at the evaporator resulted in the increase of the heat flux in all test cases. The heat pipe with a mesh wick exhibited a higher average heat flux than the thermosyphon under the same test conditions. As the mesh wick is made of copper wire, the high thermal conductivity increased as the heat load increased. As a result, the heat from the heat source in the evaporator was transferred from the pipe wall to the mesh wick and the working substance per the larger contact surface area. Thus, the working substance could easily reach the boiling point and the initial bubble boil was also distributed along the heat pipe. Also, the mesh wick allowed the condensate liquid to spread through its porosity within the condenser's surface area. Furthermore, the mesh wick also reduced the flowing speed of the condensed working substance,

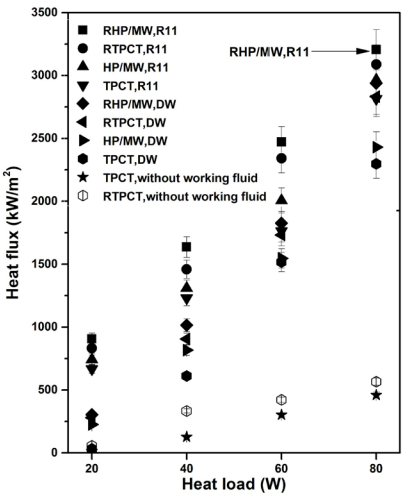

Figure 8: The relationship of heat load with heat flux.

allowing more time for the heat transfer. Therefore, for the reasons described in Figures 7 and 8, the heat pipe equipped with a mesh wick had a higher heat flux value than that of the thermosyphon tested under the same conditions. For instance, when comparing the test results between HP/MW/DW and TPCT/DW, the mean heat flux obtained from HP/MW/DW was 1255.13 kW/m^2 which was higher than TPCT/DW with an average heat flux of 1114.72 kW/m^2. Moreover, for RHP/MW/R11, the average maximum heat flux throughout the test was 2,054.57 kW/m^2. Due to RHP/MW's increased thermal and heat-emitting area, along with the mesh wick's porosity, the heat flux value obtained from the test with RHP/MW was higher than other tests under the same conditions. Upon considering in conjunction with the two-state flow patterns that occur within the RHP/MW that can be described by the wet perimeter. Therefore, a greater wet perimeter means that more heat from the heat source can be transferred to the working substance and consequently conducive to boiling. This leads to the liquidity of the dual-state flow pattern that is accompanied by the heat conduction moving from the evaporator up to the cooling condenser. The flow pattern with a higher velocity and a higher percentage of the dual-state flow pattern than the circular cross-section allows for a large amount of heat to be convected and dissipated at the condenser quickly, according to the motion of the two-state flow pattern [21]–[23]. This is the reason RHP/MW/R11 has high heat transfer and heat flux.

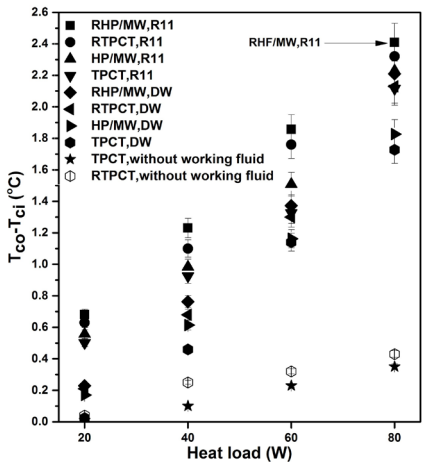

Figure 9: The relationship of heat loads and the difference of temperatures between the coolant water inlet and outlet.

3.2 *Temperature difference of outlet water and inlet temperature at condensation, ($T_{co} - T_{ci}$)*

When the heat load increased, the temperature difference between the inlet and outlet coolant water at the condenser also increased in all test cases as shown in Figure 9. Results showed that RHP/MW/R11 had a maximum temperature difference of 22.41 °C at the heat load of 80 W. RHP/MW's advantage was due to its greater areas of hear receiving and emitting of the pipe wall which enhanced heat conductivity and spread the liquid around the evaporator surface. Radial thermal conductivity through the mesh wick to the working substance resulted in a quicker boil. The mesh wick's porosity also increased the contact area at the solid-liquid interface, thus, the boiling surface area was enlarged. Using R-11 which has low boiling point, high latent heat of vaporization (R-11), and lower surface tension at a higher temperature also increased the vaporization. The continuous and consistent flow patterns together with a vigorous boiling of the working substance instigate the initial bubble flow which quickly changes to other flow patterns. A fast-moving two-state flow pattern increased the flow volume from the evaporator to the condenser which resulted in higher heat transfer [25], [26]. RHP/MW was designed to have equal shapes and sizes of the evaporator, adiabatic, and condenser sections. Together with the mesh wick, liquid film at the condenser could be distributed evenly and consistently throughout the condenser [11]–[13] thus, the heat transfer to the heat receptor was enhanced. As a result, the average temperature difference between the outlet and inlet water across the RHP/MW/R11 test was higher than in other test cases.

3.3 *The wall temperature distributions*

The temperature distribution at the pipe wall of RHP/MW and HP/MW is shown in Figure 10. Changing from round to rectangular pipe enlarged the surface areas together with the RHP/MW- mesh wick leading to higher heat transfer rate, heat flux, and the temperature difference between the outlet and the inlet water in all cases. See further details in Figures 7–9, respectively.

Temperature distribution at different points of RHP/MW and HP/MW from Figure 10(a)–(d), after transient heat transfer at the evaporator section met the conditions set forth in the initial variant, heat load at evaporator were set at 20, 40, 60, and 80 W. At the condensation for RHP/MW and HP/MW, the heat pipes were cooled by a circulating water system. The heat pipes can transfer heat from the evaporator to the condenser even with little difference in temperature between these two parts [2]. This was because the internal system of the heat pipe has been designed and constructed to provide a vacuum that facilitates the boiling of the working substance as described in Section 2.7 and Figure 4. The saturated liquid working substance contained in the evaporator section gradually begins to boil, but does not completely change to vaporization. The boils strongly increased with higher tube surface temperature of the evaporator and heat load at the evaporator section [24], [26], [27]. Therefore, as the system in this study was in a steady state, the pipe surface temperature was evenly distributed at different locations of the heat pipe, including the temperature of the inlet-outlet water at the condenser. Temperatures were recorded at various locations of the heat pipes, including RHP/MW/R11, HP/MW/R11, RHP/MW/DW, and HP/MW/DW, as shown in Figure 10(a)–(d), respectively. According to the results in all test cases, the temperature distributions at the pipe surface at different locations were similar and tended to be in the same direction. At positions 1 and 2 (evaporation section of the heat pipe), the working substance boiled and vaporized more vigorously than other sections.

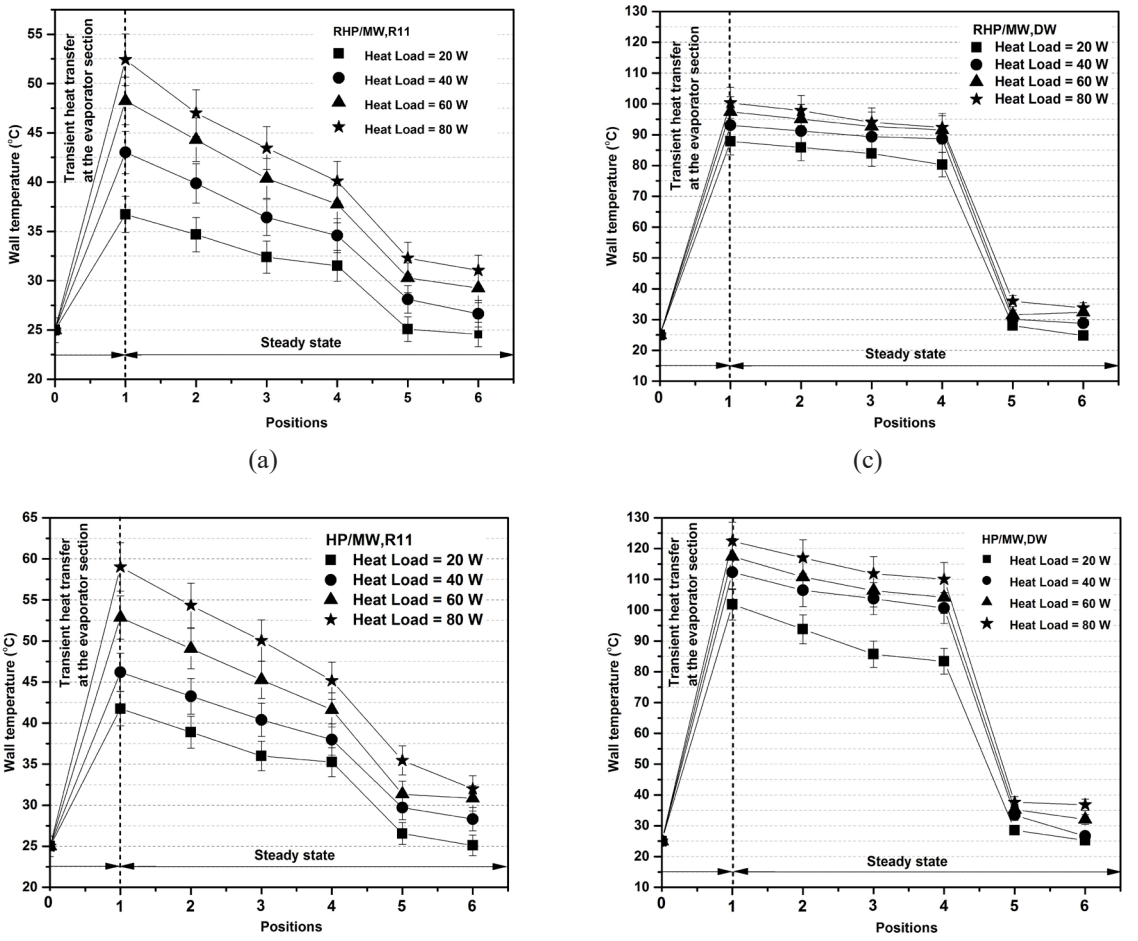

Figure 10: The pipe wall temperature distribution for RH/MW and HP/MW.

This includes the convection of heat that moved simultaneously with the two-state flow pattern. This was the area that receives direct heat from the heat source, resulting in a high pipe surface temperature before floating through the heat shield to cool down at the condenser. Then, the condensed working substance flew back to the evaporation part again. The system is characterized by a continuous cycle of operation as long as the evaporator is heated. Therefore, in every test case, the tube surface temperature distribution at different positions gradually decreased from the evaporator section (positions 1 and 2), the heat shield (positions 3 and 4), and the condensation section (positions 5 and 6) respectively. This was conducted while the test system is in steady state.

When 80 W heat load was applied, the wall temperature at the evaporator of RHP/MW/R11 over the it's entire length was the lowest at 41.05 °C. The mean wall temperature over the entire length of the pipe of HP/MW/R11, RHP/MW/DW, and HP/MW/DW were 45.99, 76.72, and 89.28 °C respectively. At the condenser of RHP, the mesh wick diffused the condensate evenly over the condenser area of the pipe wall. This led to a better latent heat transfer to the coolant circulating around the condenser [16]. Moreover, a larger surface area in RHP/MW's condenser reduced the formation of a thick liquid film by diffusing the liquid across the cooling areas. The liquid returned to the evaporator as a liquid film along the surface of the mesh wick. The enhanced condensation drove the

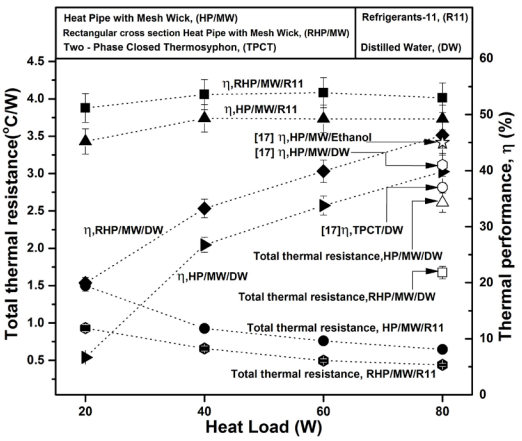

Figure 11: The relationship of heat load and total thermal resistance, and thermal performance.

liquid to the fluid basin of the working substance in the evaporator which caused the temperature to drop at the bottom surface of the evaporator. This ensured that the average surface temperature difference between the evaporator and the condenser was not greatly different [28]

3.4 *Thermal resistance (Re-c) and thermal performance*

The relationship between heat load and total thermal resistance and thermal performance as shown in Figure 11. The total thermal resistance decreased with an increase in the heat load. The trends were similar in all test cases. At low heat loads (20 and 40 W), the total thermal resistance of RHP/MW/DW and HP/MW/DW using water as a working substance was higher than 4.5 °C/W. At the heat loads of 20 and 40 W, heat transfer from the heat source to the evaporator of the heat pipe by heat conduction was not high enough to cause the working substance to boil and vaporize. This resulted in a thick liquid film within the evaporator. Thus, the rate of heat transfer of the vaporized working substance that travels to the cooling condensate was lower as well. As a result, the temperature at the tube surface of the evaporator and condenser became different. Total thermal resistance at the heat load of 20 and 40 W was high. However, the total thermal resistance reached the lowest point when the thermal load increased [16]. RHP/MW/R11 showed a small difference between the average tube surface temperature of the evaporator and the condenser, as shown in Figure 10(a). As per Section 3.1, RHP/MW/R11 had the lowest average heat resistance throughout the test at 0.6318 °C/W. Low average heat resistance is a contributing factor leading to the highest average thermal efficiency of 52.91%. This is greater than the average thermal efficiency over the entire test of HP/MW/R11, RHP/MW/DW, and HP/MW/DW which were 48.25, 34.85, and 26.75%, respectively. When comparing the thermal efficiency from the test results of [17] containing HP/MW/Ethanol, HP/MW/DW and TPCT/DW and that of RHP/MW/DW were compared, RHP/MW/DW exhibited higher thermal efficiency due to the previously mentioned thermal properties.

As per the applications and limitations of traditional heat pipes, there are different usage, depending on the suitability. Modification of the structure, greater heat receiving area and higher thermal efficiency are the crucial characteristics necessary to develop the heat pipe. Rectangular cross-section heat pipes equipped with mesh wick are another option for applications with flat contact surfaces. This reduces the limitations of traditional heat pipe applications that are mostly made of round cylindrical tubes.

4 Conclusions

This paper studied the heat transfer behavior of rectangular heat pipes with mesh wick (RHP/MW) using water and R11 as working substances. The heat loads used in the tests were 20, 40, 60, and 80 W. The results can be summarized as follows:

Changing from round to rectangular pipe had an effect on thermal reception at both the evaporator and condenser. The tests were designed to have the same wet perimeter, thus, RHP/MW showed a greater surface area for thermal reception and cooling at the evaporator and the condenser, when compared with HP/MW. The mesh wick inside the heat pipe provided more surface area for vaporization within the evaporator. This was possible due to a greater interface between the porosity of the mesh wick and the liquid state working substance. The mesh wick also created a capillary force which drew the condensed liquid in the condenser back to the evaporator for reheating. The heat pipes could distribute the liquid across the inner wall of the pipe which helped to regulate the movement of the working substance inside the heat pipe. When a

working substance with a low boiling point, high latent heat, and low surface tension are used, this allows quick and easy boiling of the saturated working substance when the condenser's temperature is increased. This influences the two-state flow patterns within the heat pipe, which directly affects the heat transfer rate and the high heat flux of the heat pipe. Therefore, R-11 was selected as a working substance which increased the heat load resulting in a higher heat transfer rate and heat flux. The increase in heat load is an important factor for heat transfer rate and heat flux. At the heat load of 80 W, the heat transfer rate and heat flux were the highest. The highest average heat transfer rate and heat flux throughout the test were achieved from RHP/MW/R11. The higher heat load resulted in a significant difference between the temperatures of the inlet and outlet coolant water at the condenser. The higher the heat load, the more heat transfer of the working substance from the evaporator to the condenser. As a result, the optimum temperature difference between the inlet and outlet coolant water was discovered when the 80 W heat load was applied. The temperature difference between the outlet and the inlet water of the RHP/MW/R11 was greater than all other test cases under the same heat load condition.

It was further found that the wall temperature distributions reduced from the evaporator to the condenser but increased when higher heat loads were applied. RHP/MW/R11 had the lowest average temperature of the pipe wall over its length. This was due to the condenser's surface area created by the mesh wick. This enhanced condensation by drawing the liquid to the working substance basin in the evaporator, resulting in a small difference in the surface temperature between the evaporator and the condenser of RHP/MW/R11 where a decrease in total thermal resistance is a critical parameter for increasing thermal efficiency. This indicated an improved relationship between the boiling and condensation behavior of the working substance in the evaporator and condenser. RHP/MW/R11 had the lowest average total thermal resistance throughout the test with the highest average thermal efficiency of 52.91%.

Finally, this research was a laboratory-based study on the effects of parameters on heat transfer characteristics of a rectangular cross-section heat pipe with mesh wick. At the laboratory scale, the production costs of RHP/MW were 6.5% higher than HP/MW. This was due to higher selling costs of rectangular cross-section pipes in the market. In this study, the control variable was the wet parameter. The maximum heat transfer rate obtained from RHP/MW/R11 was 41.98 W and the maximum heat transfer rate obtained from HP/MW/R11 was equal to 38.84 W. The obtained results serve as a foundation for future applications. The study focused on the return of investment period, by comparing the results obtained from the application of RHP/MW to HP/MW [29]. The acquired technology could be used for cooling under the solar panel which helps to increase its efficiency. Theoretical calculations showed that RHP/MW's return of investment period was 13.04% shorter than that of HP/MW. The main annual interest rate and savings (SFF, Sinking fund factor) required at the end of the usage life in order to build a heat sink of RHP/MW with solar cells next time, after the estimated useful life of 20 years, were considered. To create the future generation of RHP/MW heat sinks with solar panels, an annual accumulation of 47.46 baht per year was required. This was calculated at the interest rate of 7% percent each year. Thus, the benefits obtained from this study serve as an important baseline of thermal optimization and a guideline to optimize the RHP/MW application to the required works. This includes the works that require a flat surface area of heat receiving and cooling areas, such as solar panels, solar collector systems, as well as applications of heat exchangers that requires dehumidification or temperature reduction. The advantage of the RHP/MW, and the foundation knowledge obtained from this study, is the increased heat receiving and emitting areas.

Acknowledgments

This research work was conducted at the Thermal System Research Unit (TSR), Department of Mechanical Engineering, the Faculty of Industry and Technology, Rajamangala University of Technology Isan, Sakon Nakhon Campus, Sakon Nakhon 47160, Thailand.

References

[1] S. Sichamnan, T. Chompookham, and S. Rittidech, "Efficiency enhancement of solar panels using copper mesh wick heat pipe," *UBU Engineering Journal*, vol. 9, no. 1, pp. 11–22, 2016.

[2] R. Sampan, *Advanced Heat Pipe*. Maha Sarakham, Thailand: Apichat Printing, 2013.
[3] A. Rodbumrung, "Influence of corrosion on the thermal performance and life time of heat pipe with sintered wick," Ph.D. dissertation, Faculty of Engineering, Mahasarakham University, Maha Sarakham, 2016.
[4] P. Naphon, "On the performance of air conditioner with heat pipe for cooling air in the condenser," *Energy Conversion and Management*, vol. 51, no. 11, pp. 2362–2366, 2010.
[5] L. L. Vasiliev, "Micro and miniature heat pipes – Electronic component coolers," *Applied Thermal Engineering*, vol. 28, no. 4, pp. 266–273, 2008.
[6] H. Akachi, F. Polasek, and P. Stulc, "Pulsating heat pipes," in *the 5th International Heat Pipe Symposium*, 1996, pp. 208–217.
[7] W. Srimuang, P. Khantikomol, and B. Krittacom, "An experimental investigation of effectiveness of a closed-end flat heat pipe heat exchanger," *KKU Engineering Journal*, vol. 40, no. 1, pp. 21–27, 2013.
[8] L. G. Asirvatham, R. Nimmagadda, and S. Wongwises, "Heat transfer performance of screen mesh wick heat pipes using silver–water nanofluid," *International Journal of Heat and Mass Transfer*, vol. 60, pp. 201–209, 2013.
[9] P. Naphon, P. Assadamongkol, and T. Borirak, "Experimental investigation of titanium nanofluids on the heat pipe thermal efficiency," *International Communications in Heat and Mass Transfer*, vol. 35, no. 10, pp. 1316–1319, 2008.
[10] K. H. Do and S. P. Jang, "Effect of nanofluids on the thermal performance of a flat micro heat pipe with a rectangular grooved wick," *International Journal of Heat and Mass Transfer*, vol. 53, no. 9–10, pp. 2183–2192, 2010.
[11] P. Amatachaya and W. Srimuang, "Comparative heat transfer characteristics of a flat two-phase closed thermosyphon (FTPCT) and a conventional two-phase closed thermosyphon (CTPCT)," *International Communications in Heat and Mass Transfer*, vol. 37, no. 3, pp. 293–298, 2010.
[12] N. Bhuwakietkumjohn and T. Parametthanuwat, "Heat transfer behaviour of silver particles containing oleic acid surfactant: Application in a two phase closed rectangular cross sectional thermosyphon (RTPTC)," *Heat and Mass Transfer*, vol. 53, no. 1, pp. 37–48, 2016.
[13] W. Srimuang, S. Rittidech, and B. Bubphachot, "Heat transfer characteristics of a vertical flat thermosyphon (VFT)," *Journal of Mechanical Science and Technology*, vol. 23, no. 9, pp. 2548–2554, 2009.
[14] F. P. Incropera and D. P. DeWitt, *Fundamentals of Heat and Mass Transfer*. Michigan: Wiley, 1996.
[15] H. Li, F. Jiang, G. Qi, and X. Li, "Investigation of the thermal performance of a novel thermosyphon combined with fluidized bed heat transfer technology," *Powder Technology*, vol. 374, pp. 40–48, 2020.
[16] K. H. Do, H. J. Ha, and S. P. Jang, "Thermal resistance of screen mesh wick heat pipes using the water-based Al_2O_3 nanofluids," *International Journal of Heat and Mass Transfer*, vol. 53, no. 25–26, pp. 5888–5894, 2010.
[17] S. Satitpong, B. Supattra, and R. Sampan, "Study of parameters have effected to the heat pipe with mesh wick," *RMUTP Research*, vol. 12, no. 2, pp. 172–183, 2018.
[18] M. M. Sarafraz, O. Pourmehran, B. Yang, and M. Arjomandi, "Assessment of the thermal performance of a thermosyphon heat pipe using zirconia-acetone nanofluids," *Renewable Energy*, vol. 136, pp. 884–895, 2019.
[19] M. Kaya, "An experimental investigation on thermal efficiency of two-phase closed thermosyphon (TPCT) filled with CuO/water nanofluid," *Engineering Science and Technology, an International Journal*, vol. 23, no. 4, pp. 812–820, 2020.
[20] P. H. D. Santos, K. A. T. Vicente, L. Santos Reis, L. S. Marquardt, and T. A. Alves, "Modeling and experimental tests of a copper thermosyphon," *Acta Scientiarum Technology*, vol. 39, no. 1, pp. 59–68, 2017.
[21] P. Thanya, R. Sampan, P. Adisak, Y. Ding, and S. Witharana, "Application of silver nanofluid containing oleicacid surfactant in a thermosyphon economizer," *Nanoscale Research Letters*, vol. 6, 2011, Art. no. 315.
[22] D. Reay and P. Kew, *Heat Pipe, Theory, Design and Application*, 5th ed. Oxford, UK: Butterworth-Heinemann, 2006.
[23] A. Faghri, *Heat Pipe Science and Technology*. Washington, DC: Taylor & Francis, 1995.

[24] P. Terdtoon, *Boiling*. Chiang Mai, Thailand: Chiang Mai University, 2001.
[25] C. Piyanun, *Heat Pipe Technologies*. Phitsanulok, Thailand: Focus Printing, 2012.
[26] S. Sichamnan, "Flow patterns and heat transfer characteristic of two-phase closed rectangular cross sectional area thermosyphon," Ph.D. dissertation, Department of Mechanical Engineering, Faculty of Engineering, Mahasarakham University, Maha Sarakham, 2019.
[27] T. Chompookham, S. Sichamnan, N. Bhuwakietkumjohn, and T. Parametthanuwat, "The rectangular two-phase closed thermosyphon: A case study of two-phase internal flow patterns behaviour for heat performance," *Archives of Thermodynamics*, vol. 41, no. 3, pp. 223–254, 2020.
[28] S. V. Mutalikdesai and A. M. Kate, "Experimental investigation of an aluminium thermosyphon at normal operating conditions," *Journal of Thermal Engineering*, vol. 6, no. 5, pp. 724–735, 2020.
[29] S. Sichamnan, "A mathematic model of photovoltaic solar collectors by heat pipe installation," M.S. thesis, Department of Mechanical Engineering, Faculty of Engineering, Mahasarakham University, Maha Sarakham, 2015.